Integrated plasmonic waveguides: A mode solver based on density of states formulation

Gérard Colas des Francs,* Jonathan Grandidier, Sébastien Massenot,† Alexandre Bouhelier, Jean-Claude Weeber, and Alain Dereux

Institut Carnot de Bourgogne, UMR 5209, CNRS–Université de Bourgogne, 9 Av. A. Savary, BP 47 870, 21078 Dijon, France

(Received 2 June 2009; revised manuscript received 6 August 2009; published 17 September 2009)

We express the density of states (DOS) near guided resonances of plasmonic waveguides by using multiple-scattering theory. In direct analogy with the case of localized electronic defect states in condensed matter, we demonstrate that optical DOS variations follow a lorentzian profile near guided modes resonances. The lorentzian shape gives quantitative information on the guided modes (effective index, propagation length, and polarization state). We numerically investigate both leaky and bound (lossy) modes supported by dielectric-loaded surface-plasmon-polariton waveguides.

DOI: 10.1103/PhysRevB.80.115419 PACS number(s): 73.20.Mf, 42.25.Bs, 73.21.−b, 42.82.Et

I. INTRODUCTION

Optical integrated circuits are widely used since the 1960s due to their high ability for data communications at small cost. A widely used configuration consists of a strip of dielectric material deposited on top of a planar waveguide. This structure is called a strip-loaded waveguide. The dielectric strip leads to a lateral mode confinement into the planar waveguide.[1] Since the mode does not overlap the loading strip boundaries, scattering losses by the strip corners are limited. Moreover, depending on the dielectric material (polymer, semiconductor, nonlinear glass,…), various optical devices are achievable.[1] In addition, metallic electrodes can also be used as loading strip lines with useful applications for designing electro-optical devices.[1] Recently, the concept of dielectric-loaded surface-plasmon-polariton waveguide (DLSPPW) has been proposed. This configuration, comprised of a dielectric material strip deposited onto a metal film, optimizes the opportunities of combining electrical and optical properties.[2–4] Very recently, we demonstrated loss compensation in strongly confined DLSPPW, in direct analogy with integrated optical amplifier.[5] To this purpose, the dielectric load was made of a polymer strip doped with quantum dots, and played the role of gain medium under optical pumping. Other dielectric materials have to be developed to manage all-optical integrated devices. In particular, ultrafast photonic circuits can be achieved using nonlinear materials such as chalcogenide glasses.[6] These glasses have high-linear indices so that chalcogenide-DLSPPW support bound modes. However, these bound modes are not easily accessible using, e.g., differential method which was recently adapted to the DLSPPW configuration.[7]

Therefore, we develop here a mode solver based on density-of-states formulation, available for two-dimensional (2D) waveguides of arbitrary shape and nature. This formulation is directly inspired by the study of localized electronic defects and impurities in condensed matter. Indeed, the electronic density of states presents then a Breit-Wigner (lorentzian) form near scattering resonances, characterizing the scattering channel involved in the process.[8] We will profit here of the strong analogy between light and electronic scattering formalisms[9,10] to fully characterize a guided mode throughout the optical density of states associated to the wave-guiding structure.

The paper is organized as follows. Section II will present the theoretical framework. Numerical simulations are reported in Sec. III for the example of a leaky mode already extensively investigated in the literature. Finally, Sec. IV considers bound modes supported by a high index material.

II. THEORETICAL BACKGROUND

The main idea of this paper is to work with the optical density of states (DOS) of the wave-guiding structure. In this first section, we briefly summarize DOS definition and properties, useful for characterizing integrated photonic waveguides. Without loss of generality, we focus on the DLSPPW configuration, described in Fig. 1(a). A dielectric load locally modifies the optical index near a metallic film deposited on a substrate. Such a configuration is well known to support a surface-plasmon-polariton mode, laterally confined at the metal/dielectric interface.[2,3] Due to the translational invariance along y axis, the wave-vector component k_y is a constant of the system that characterizes a guided mode. The electromagnetic density of states $\rho(k_y;\omega)$ is the density of electromagnetic modes in the wave-vector interval $[k_y, k_y + dk_y]$ at fixed frequency ω. Since $v=k_y^2$ is the eigenvalue of the wave equation, it is easier to work with $\tilde{\rho}(k_y^2;\omega) = (2k_y)^{-1}\rho(k_y;\omega)$ that is related to the wave equation kernel (2D-Green's dyad) $\mathbf{G}$ associated to the system by[9,11,12]

$$\tilde{\rho}(k_y^2;\omega) = -\frac{1}{\pi}\mathrm{Im\ Tr}[\epsilon\mathbf{G}(k_y;\omega)] = \frac{d}{dv}\left\{\frac{1}{\pi}\mathrm{Im\ ln}[\det\ \epsilon\mathbf{G}(k_y;\omega)]\right\}. \quad (1)$$

This relation has to be manipulated with care since it holds

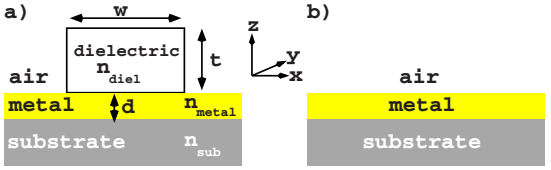

FIG. 1. (Color online) (a) DLSPPW configuration. A dielectric ridge [thickness t, width w, optical index $n_{diel}=(\epsilon_{diel})^{1/2}$] is deposited on a metal film of thickness d and optical index $n_{\mathrm{metal}}=(\epsilon_{\mathrm{metal}})^{1/2}$. The substrate index is $n_{sub}=(\epsilon_{sub})^{1/2}$. (b) Reference system: substrate/metal/air slab. See text for details.

only in the region where $\epsilon(\mathbf{r})$ does not change sign so that Sturm-Liouville theory applies.[13] Since metallic film possesses a negative dielectric constant, it is convenient to restrict the domain of investigation on the dielectric strip only. Moreover, the Dyson's equation expresses the Green's dyad $\mathbf{G}$ of any arbitrary system as a function of the Green's dyad $\mathbf{G}_{ref}$ of a reference system[12]

$$\mathbf{G} = [\mathbf{I} - \mathbf{G}_{ref}V]^{-1}\mathbf{G}_{ref}, \tag{2}$$

where $V=k^2(\epsilon_{ref}-\epsilon_{obj})$ represents the perturbation due to the object $(k=\omega/c)$. In our case, we choose the substrate/metal/air slab system described in Fig. 1(b) as the reference system, so that $V=k^2(1-\epsilon_{diel})$ inside the dielectric strip and is null elsewhere. Then, the variation in DOS due to the guiding structure can be written as[14]

$$\Delta\tilde{\rho}(k_y^2;\omega) = \tilde{\rho}(k_y^2;\omega) - \tilde{\rho}_{ref}(k_y^2;\omega)$$
$$= -\frac{1}{\pi}\frac{d}{dv}\mathrm{Im}\ \ln[D(k_y;\omega)], \quad \text{with} \tag{3}$$

$$D(k_y;\omega) = \det[\mathbf{I} - \mathbf{G}_{ref}V]. \tag{4}$$

The presence of V in Eq. (4) indicates an implicit integration over the perturbation surface. Applying then standard procedure for multiple-scattering description, one can demonstrate that the DOS variation has a lorentzian shape near a resonance.[8] For this purpose, we express DOS variations in terms of the scattering phase shift $\theta(k_y;\omega)=-\arg[D(k_y;\omega)]$,

$$\Delta\tilde{\rho}(k_y^2;\omega) = \frac{1}{\pi}\frac{d\theta}{dv}. \tag{5}$$

This expression is analogous to the electronic DOS derivation $n(E)=dN(E)/dE$ with $N(E)$ being the number of electronic modes at the energy E. Therefore, θ/π can be seen as the number of electromagnetic modes created in presence of the guiding structure. Due to a change in Riemann sheet, θ varies of π around $\mathrm{Re}[D(k_{y0};\omega)]\approx 0$. After a Taylor expansion of $\mathrm{Re}[D(k_y;\omega)]$ near $v_0=k_{y0}^2$, we obtain, following a procedure similar to that described in Ref. 8,

$$\Delta\tilde{\rho}(k_y^2;\omega) \approx \frac{g}{\pi}\frac{\Gamma/2}{(k_y^2-k_{y0}^2)^2+(\Gamma/2)^2}, \quad \text{with}$$

$$\Gamma = 2\frac{\mathrm{Im}\ D(k_y;\omega)}{[d\ \mathrm{Re}\ D(k_y;\omega)/dv]_{v_0}}, \tag{6}$$

where g is the waveguide degeneracy at ω and k_{y0}^2. Remembering that $v=k_y^2$, we can now express the DOS variation $\Delta\rho(k_y;\omega)=2k_y\Delta\tilde{\rho}(k_y^2;\omega)$ near a resonance,

$$\Delta\rho(k_y;\omega) \approx \frac{2gk_{y0}}{\pi}\frac{\Gamma/2}{(k_y^2-k_{y0}^2)^2+(\Gamma/2)^2}, \tag{7}$$

$$\approx \frac{g}{\pi}\frac{\Delta k_y/2}{(k_y-k_{y0})^2+(\Delta k_y/2)^2}, \quad \text{with} \quad \Delta k_y = \frac{\Gamma}{2k_{y0}}, \tag{8}$$

where we use $(k_y^2-k_{y0}^2)\approx 2k_{y0}(k_y-k_{y0})$ near k_{y0}.[15]

To summarize, the variation in the density of states presents a lorentzian form near a guided wave-vector resonance k_{y0}, in exact analogy with the Breit-Wigner (lorentzian) profile followed by the *electronic* density of states in presence of a localized electronic defect. The optical resonance full width at half maximum (FWHM) Δk_y gives the mode propagation length $L_{\mathrm{SPP}}=1/\Delta k_y$. Additionally, the number of supported mode is $N(\omega)=\int dk_y\Delta\rho(k_y;\omega)=g$. Obviously, the density of created modes is maximum at the resonance and is $\Delta\rho(k_{y0},\omega)=2gL_{\mathrm{SPP}}/\pi$. In case of DLSPPW configuration, this simple relation shows that *a mode can be supported if and only if its propagation length is long enough* since the collective oscillation of electrons has to establish. Equivalently, the DOS variations can be expressed as a function of ω.[16] The maximum DOS difference expresses then $\Delta\rho(k_{y0},\omega_0)=2g\tau/(\pi v_g)$, where τ is the mode lifetime and $v_g=\partial\omega/\partial k_y$ is the mode group velocity. Again, this means that the mode need sufficient time to establish (see also section 9.4.1 of Ref. 17).

Knowing the mode wave vector k_{y0} and propagation length L_{SPP}, the mode electric field is computed thanks to the Green's dyad as

$$\mathbf{E}(r_\parallel,t) = \mathbf{E}_{2\mathrm{D}}(r_\parallel)e^{i(k_{y0}y-\omega t)}e^{-y/L_{\mathrm{SPP}}}, \quad \text{with} \tag{9}$$

$$\mathbf{E}_{2\mathrm{D}}(\mathbf{r}_\parallel) = \mathbf{G}(\mathbf{r}_\parallel,\mathbf{r}_\parallel^{\mathbf{0}},k_{y0})\cdot\mathbf{p} - \mathbf{G}_0(\mathbf{r}_\parallel,\mathbf{r}_\parallel^{\mathbf{0}},k_{y0})\cdot\mathbf{p}, \tag{10}$$

where $\mathbf{r}_\parallel=(x,z)$ represents the coordinates in the (XZ) plane and $\mathbf{p}$ is a 2D dipoles line source, located at an arbitrary place $\mathbf{r}_\parallel^{\mathbf{0}}$ near the waveguide, used to excite the mode. $\mathbf{G}_0(\mathbf{r}_\parallel,\mathbf{r}_\parallel^{\mathbf{0}},k_{y0})$ is the free-space Green's dyad so that the second term in the right-hand side of Eq. (10) removes the excitation field and expression (10) gives the mode field only.

It is worth noting that we do not use expression (3) to evaluate DOS difference since it leads to numerical instabilities because of the difficulty to properly choose the Riemann sheet where the scattering phase shift $\theta(k_y,\omega)$ is defined. Instead, we go back to the generic expression (1). Practically, DOS variation in presence of the waveguide is numerically calculated by

$$\Delta\rho(k_y;\omega) = -\frac{2k_y}{\pi}\mathrm{Im}\int d\mathbf{r}_\parallel[\epsilon(\mathbf{r}_\parallel)\mathbf{G}(\mathbf{r}_\parallel,\mathbf{r}_\parallel,k_y,\omega)$$
$$-\epsilon_{ref}(\mathbf{r}_\parallel)\mathbf{G}_{ref}(\mathbf{r}_\parallel,\mathbf{r}_\parallel,k_y,\omega)], \tag{11}$$

Since we are interested in the waveguide modes, *confined inside the object*, we can limit the integration to the object only.[12] Last, due to the vectorial nature of the electromagnetic field, one interestingly defined *partial* DOS variations as[18,19]

$$\Delta\rho_i(k_y;\omega) = -\frac{2k_y}{\pi}\mathrm{Im}\int d\mathbf{r}_\parallel[\epsilon(\mathbf{r}_\parallel)G_{ii}(\mathbf{r}_\parallel,\mathbf{r}_\parallel,k_y,\omega)$$
$$-\epsilon_{ref}(\mathbf{r}_\parallel)G_{ref,ii}(\mathbf{r}_\parallel,\mathbf{r}_\parallel,k_y,\omega)], (i=x,y,z). \tag{12}$$

The Green's dyad is numerically calculated as described in Ref. 20.

III. LEAKY MODES

In this section, we demonstrate the reliability of our approach by considering leaky modes supported by a DL-

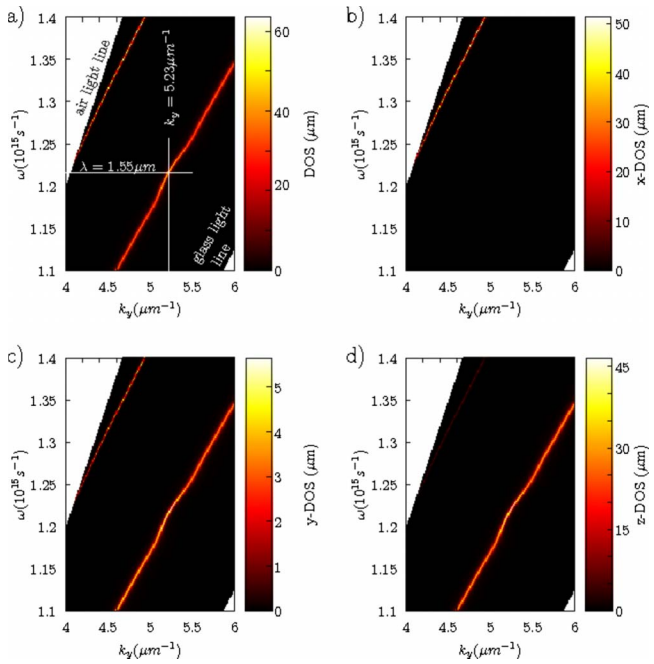

FIG. 2. (Color online) (a) DOS variations calculated for a DLSPPW. The white lines indicate the fundamental mode propagation constant at telecom wavelength $\lambda=1.55\mu$m. The dispersion curve slope gives a group velocity $v_g/c=0.6$ at this wavelength. This mode is extensively studied in the following. Panels (b), (c), and (d) show the x-, y-, and z-DOS contributions to the total DOS variation, respectively (note the different scales). The structure is made of a 600 nm$\times$600 nm PMMA strip deposited on a 100 nm gold film. Dielectric constants are taken from Ref. 24.

SPPW. These modes have been already theoretically studied using either effective index model,[3] finite element numerical simulations,[3,4,21] or differential method[7] and experimentally investigated by both near-field[22] and leakage radiation microscopies.[5,23]

A. Single mode waveguide

1. Dispersion relation

The DLSPPW characteristics are optimized as indicated in Ref. 3 for the telecom wavelength $\lambda=2\pi c/\omega=1.55$ μm. The gold film is $d=100$ nm thick and the polymethylmethacrylate (PMMA) ridge thickness and width are $t=w=600$ nm. Figure 2 represents the waveguide modes dispersion around telecom wavelength. Below $\omega=1.23\times10^{15}$ s^{-1} ($\lambda=1.53$ μm), the waveguide is monomodal. Apart for $k_y=0$, one cannot separate transverse electric (TE) and transverse magnetic (TM) polarization in partial DOSs.[12,20] However, z-DOS is clearly preponderant [Fig. 2(d)], indicating that TM polarization is concerned. The dispersion relation of this fundamental TM_{00} mode is in good agreement with the Fig. 1c of Ref. 4. The first-excited mode also appears in Fig. 2(a). It is the TE_{00} mode as confirmed using the differential method and noticing the main contribution of the x-DOS [Fig. 2(b)].

In the following, we fix the wavelength to $\lambda=1.55$ μm. The guided SPP mode (TM_{00}) propagation constant is k_{y0}

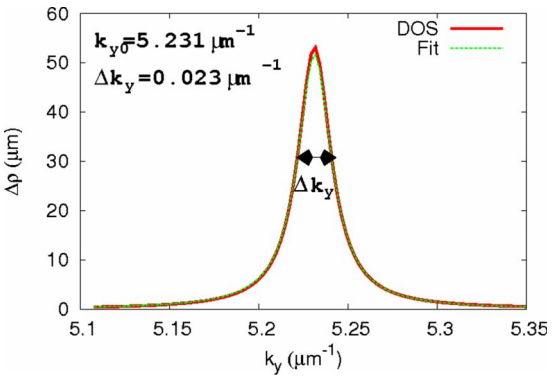

FIG. 3. (Color online) Cross section of dispersion relation (Fig. 2) at given frequency (corresponding to $\lambda=1.55$ μm). Fit curve is a lorentzian fit [Eq. (8)] with parameters indicated on the figure.

$=5.23$ μm^{-1} at $\lambda=1.55$ μm. The DOS variation, presented on Fig. 3, perfectly matches a lorentzian profile as expected from Eq. (8). The curve FWHM $\Delta k_y=0.023$ μm^{-1} corresponds to a propagation length $L_{SPP}=1/\Delta k_y=43$ μm. We also calculate the DOS variation versus ω at fixed $k_y=5.23$ μm^{-1} (not shown) and obtain a lorentzian profile with a FWHM $\Delta\omega=3.96\times10^{12}$ s^{-1} giving a mode lifetime $\tau=1/\gamma=252$ fs.[16] Group velocity satisfies $v_g=L_{SPP}/\tau=0.57c$, in good agreement with the dispersion slope in Fig. 2.

2. Mode effective index at telecom wavelength

In the following, we work at fixed frequency so that Eq. (8) is rewritten,

$$\Delta\rho(k_y;\omega)\approx\frac{g}{\pi k_0}\frac{n''}{(k_y/k_0-n_{eff})^2+n''^2},\quad \text{with } n''=(\Delta k_y/2k_0) \tag{13}$$

where $n_{eff}=k_{y0}/k_0$ is the mode effective index. n'' is defined so that the mode complex effective index is written as $\tilde{n}_{\text{eff}}=n_{eff}+in''$. The mode propagation length is then $L_{SPP}=\lambda/4\pi n''$. Since an image recorded in the Fourier plane by leakage radiation microscopy is easily calibrated in effective indices, it is advantageously compared with expression (13).[23,25] Specifically, it presents the same Lorentzian profile (apart from amplitude).[5]

Figure 4(a) represents the partial DOSs variations. A resonance clearly appears at $k_y/k_0=1.291$. As indicated previously, the z-DOS is clearly preponderant near the resonance since the mode is TM polarized. There is also a nonnegligible y-DOS contribution as expected for a *longitudinal* plasmon mode. We deduce the mode effective index $n_{eff}=1.291$ and propagation length $L_{SPP}=\lambda/(4\pi n'')=43.2$ μm ($n''=2.85\times10^{-3}$), in agreement with previous studies.[3,7,21] The guided mode is also characterized considering a TM polarized 2D Gaussian excitation. The mode intensity decaying in the near-field of the waveguide clearly appears in Fig. 4(b). An exponential fit gives $L_{SPP}^{2D}=44.4$ μm. Note that the difference between the propagation lengths deduced from DOS FWHM and from Gaussian beam propagation originates from three-dimensional (3D) and 2D mode shapes.[21] Importantly, the exact 3D mode characteristics associated

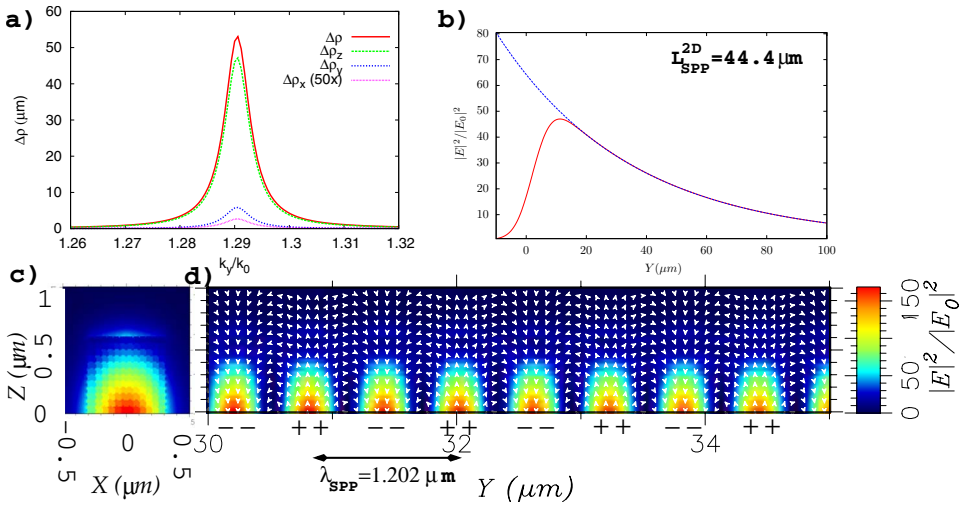

FIG. 4. (Color online) Single waveguide characterization. (a) Partial DOSs calculated as a function of k_y/k_0. x-DOS is magnified 50× to be visible. (b) (Time-averaged) electric intensity calculated 50 nm above the dielectric ridge when the system is excited by a (2D-) Gaussian beam by total internal reflection from the substrate centered at incident angle $\arcsin(n_{eff}/n_{sub})=53.8°$. The blue curve is an exponential fit with decay length $L_{\mathrm{SPP}}^{\mathrm{2D}}=44.4$ μm. (c) Mode intensity pattern $\mathbf{E}_{\mathrm{2D}}(\mathbf{r}_{\parallel})$. (d) Electric field intensity computed at a certain time, far from the incident excitation spot [see Fig. 4(b)], revealing the mode propagation. The white arrows indicate the electric field orientation. "−−" and "++" represent the charges density signs at the metal surface, deduced from the field polarization. The dielectric ridge ($n_{diel}=1.535$) is $t=600$ nm thick and $w=600$ nm width. The gold film and glass substrate optical indices are $n_{\mathrm{metal}}=0.55+i11.5$ and $n_{sub}=1.6$, respectively. Incident vacuum wavelength is $\lambda=1.55$ μm. Electric intensity is normalized with respect to the incident intensity at the focal point ($y=0, z=0$).

with the 2D waveguide are obtained through DOS shape. The mode pattern, calculated in Fig. 4(c), demonstrates the good confinement.[23] Finally, the mode intensity at a given time is shown in Fig. 4(d). The collective charge oscillation, mode enhancement, and confinement at the metal/dielectric interface typical from a surface-plasmon mode are visible. The plasmon mode wavelength $\lambda_{\mathrm{SPP}}=1.202$ $\mu\mathrm{m}=\lambda/n_{eff}$ is again consistent with $n_{eff}=1.29$.

B. Coupling strength

In order to demonstrate the versatility and efficiency of DOS formulation as a mode solver, we now investigate coupling strength between two identical waveguides. The DOS variation for two DLSPPWs separated by 500 nm (edge to edge) is presented in Fig. 5(a). Comparing DOS amplitudes in Figs. 5(a) and 3, it appears that no new mode is created but modes coupling breaks the degeneracy as expected. Due to the coupling between the two isolated waveguide modes, a symmetric and antisymmetric supermodes appear at effective index $n_{\mathrm{eff}}^{s}=1.309$ and $n_{\mathrm{eff}}^{a}=1.269$, respectively. These two modes present identical propagation length $L_{\mathrm{SPP}}^{s}=L_{\mathrm{SPP}}^{a}=(\lambda/4\pi n'')=41.4$ μm, slightly below the isolated waveguide mode propagation length since some additional leakages occur during energy transfer to the nearby waveguide. Finally, the coupling length between the two waveguides obeys

$$L_C=\frac{\lambda}{2(n_{\mathrm{eff}}^{s}-n_{\mathrm{eff}}^{a})}. \tag{14}$$

We obtain $L_C=19.2$ μm for $d=500$ nm. We again compare this result with the direct calculation considering excitation of one of the two guides. The electric intensity shown on Fig. 5(b) presents typical oscillation due to energy transfer from one guide to the other. The coupling length is in excellent agreement with the number obtained previously. Figure 5(b) represents the supermodes effective indices as a function of guide separation distance. Finally, the evanescent coupling between the two waveguides, follows an exponential law with a lateral wave-vector component $k_x=1/290$ nm^{-1} [Fig. 5(c)], in good agreement with finite element study done in Ref. 21, and indicating a strong field confinement near the guide.

We would like to draw a temporary conclusion here. The DOS computation in presence of a complex wave-guiding structure allows direct and complete characterization of the supported mode: propagation constant and length, as well as polarization state. In addition coupling between two waveguides is also easily described.

IV. BOUND MODES

In this last section, we apply the DOS method to bound (lossy) modes. The modes investigated above have effective indices below the substrate optical index so that they radiatively leak into the substrate. In order to improve the mode confinement, we now investigate bound modes in DLSPPW. They are characterized by effective indices higher than substrate and superstrate (air) optical indices and can be obtained with high index dielectric materials. In this section, we consider a dielectric strip of optical index $n=2.437$ that corresponds for instance to chalcogenide glasses[26] or BM4i4i polymer, two materials that present strong nonlinear properties promising for all-optical integrated photonic.[6]

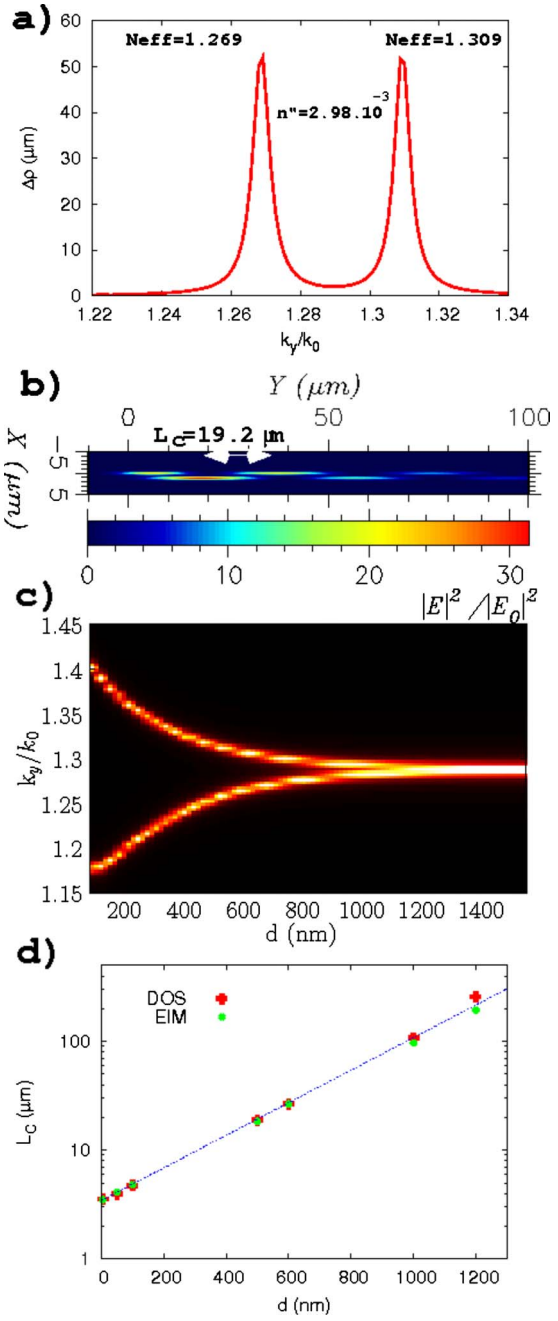

FIG. 5. (Color online) Coupled DLSPPWs. (a) DOS difference computed for two guides separated by $d=500$ nm (edge to edge). (b) Electric intensity calculated 50 nm above the DLSPPWs when the top waveguide is excited with a (spatially truncated) 2D-Gaussian beam at incident angle 53.8°. (c) Coupled waveguides DOS as a function of separation distance. (d) Coupling length for several separation distance deduced from DOS variations ("DOS") or effective index model ("EIM"). The dotted line is an exponential fit with a slope $k_x=1/290$ nm^{-1}.

Using effective index model, we first roughly determine the strip thickness and width that optimize the mode confinement and ensure monomodal conditions.[3,23] We found that a strip with square section of 300 nm side allows for a good mode confinement, and supports a single mode (TM_{00}). We deduce from DOS variation [Fig. 6(a)] the mode effective

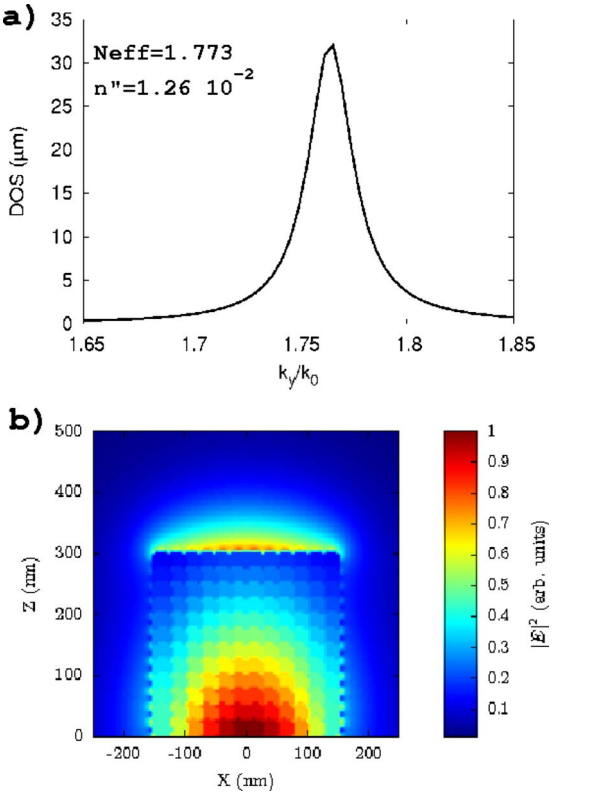

FIG. 6. (Color online) (a) DOS variation for a high index ($n=2.437$) strip above a 50 nm gold film. (b) Mode intensity profile in the (XZ) plane.

index ($n_{eff}=1.773$) and propagation length ($L_{SPP}=9.8$ μm). The mode profile, represented in Fig. 6(b) is similar to PMMA leaky mode [Fig. 4(c)]. However, although being a bound mode (effective index higher than the substrate index), this mode has a very low propagation length compared to the leaky PMMA mode. This is due to the high dielectric index that *pushes* the mode field into the lossy metal. This can be clearly seen considering thin gold films. Figure 7 represents the mode profile for leaky and bound modes for two gold thicknesses. As the gold film thickness decreases, radiatives losses of the leaky modes into the substrate increase so that the PMMA-DLSPPW mode propagation length drops to $L_{SPP}=1.5$ μm for 10 nm gold film [Fig. 7(b)]. In case of bound mode, no radiative loss is observed [Fig. 7(d)] but due to the high mode effective index, strong mode penetration into the lossy gold film is visible so that rather low propagation length ($L_{SPP}=1.4$ μm) is also obtained.

Finally, this study shows that one has to avoid high index materials for DLSPPW application, in contrast to standard dielectric integrated waveguides.[27] Figure 8(a) also compares effective indices obtained using approximated effective index model[3] and two exact numerical methods, namely, the differential method and the DOS variations. Numerical methods are in excellent agreement for leaky modes. Bound modes cannot be easily investigated by the differential method since it generally relies on mode excitation through the substrate,[7] but they are accessible using DOS formulation. The agreement is within 10% as far as propagation length is concerned [Fig. 8(b)].

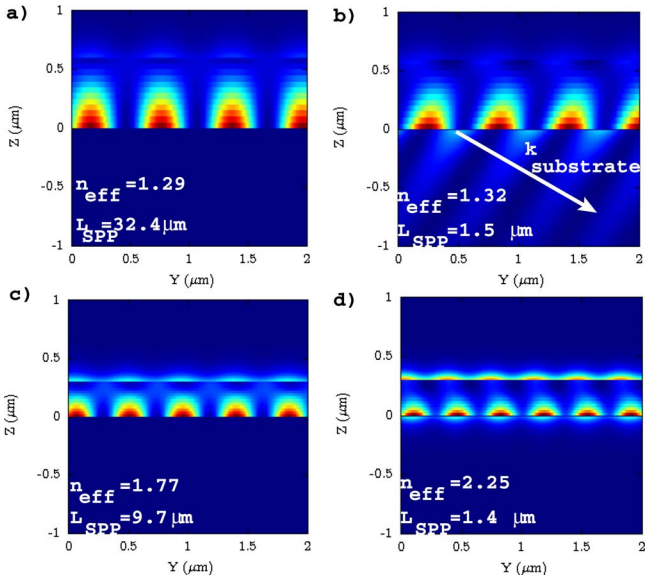

FIG. 7. (Color online) Mode intensity profile in the (*YZ*) plane for (a,b) PMMA ($t=w=600$ nm) and (c,d) chalcogenide ($t=w=300$ nm) DLSPPW. The gold film thickness is (a,c) 50 nm or (b,d) 10 nm. The vacuum wavelength is $\lambda=1.55$ μm. In (b), $k_{\text{substrate}}$ represents the leaky mode wave vector into the substrate. The mode effective indices and propagation length obtained from DOS calculation are indicated on the figures.

V. CONCLUSION

In conclusion, the evaluation of density of modes modification in presence of a photonic wave-guiding structure allows direct estimation of both mode effective index and propagation length for either leaky and bound modes. Moreover, a close inspection of partial DOSs, which build up the density of modes, directly reveals the mode polarization state. Finally, it is worthwhile noting that although we investigated a specific configuration, namely, DLSPPW, this method is general and is available for any 2D guiding structure. Last, we would like to mention that this method intrinsically concerns lossy modes. In case of absolutely no loss (neither by leakage, absorption, nor corners scattering), it could be applied by artificially adding an extremely small absorption to the waveguide.

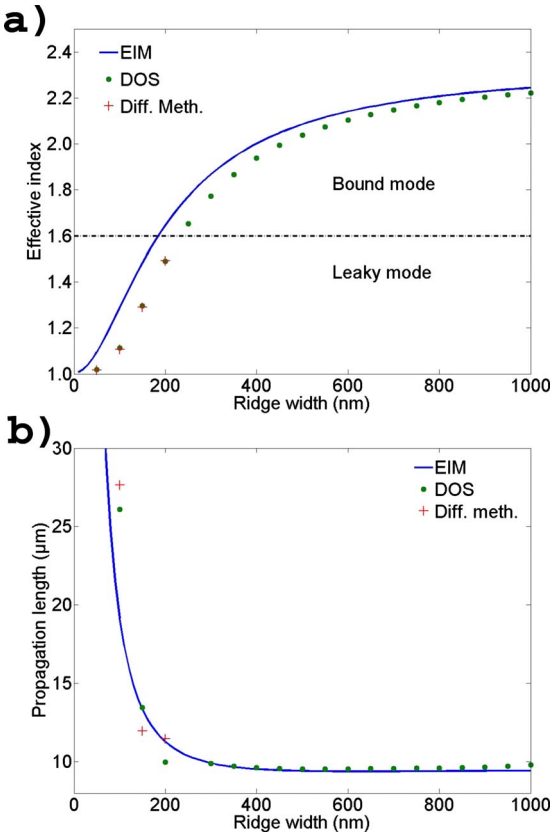

FIG. 8. (Color online) Comparison of the (a) effective indices and (b) propagation length obtained with either effective index model, differential method, or DOS calculation. The chalcogenide strip thickness is 300 nm and its width varies from 0 to 1 μm. In (a), the horizontal line at the substrate index separates bound and leaky modes.

ACKNOWLEDGMENTS

The authors gratefully acknowledge F. Smektala for fruitful discussion on chalcogenide glass properties. This work is supported by the European Commission (project PLASMOCOM, Grant No. EC FP6 IST 034754 STREP).

*gerard.colas-des-francs@u-bourgogne.fr
†Present address: Institut Supérieur de l'Aéronautique et de l'Espace, Toulouse, France.

[1] R. G. Hunsperger, *Integrated Optics: Theory and Technology* (Springer, New York, 2002).
[2] B. Steinberger, A. Hohenau, H. Ditlbacher, A. L. Stepanov, A. Drezet, F. R. Aussenegg, A. Leitner, and J. R. Krenn, Appl. Phys. Lett. **88**, 094104 (2006).
[3] T. Holmgaard and S. I. Bozhevolnyi, Phys. Rev. B **75**, 245405 (2007).
[4] A. V. Krasavin and A. V. Zayats, Phys. Rev. B **78**, 045425 (2008).
[5] J. Grandidier, G. Colas des Francs, S. Massenot, A. Bouhelier, L. Markey, J. Weeber, C. Finot, and A. Dereux, Nano Lett. **9**, 2935 (2009).
[6] V. Ta'eed *et al.*, Opt. Express **15**, 9205 (2007).
[7] S. Massenot, J.-C. Weeber, A. Bouhelier, G. Colas des Francs, J. Grandidier, L. Markey, and A. Dereux, Opt. Express **16**, 17599 (2008).
[8] J. Callaway, *Quantum Theory of the Solid State* (Academic Press, New York, 1976).
[9] A. Lagendijk and B. Tiggelen, Phys. Rep. **270**, 143 (1996).
[10] G. Colas des Francs, C. Girard, J.-C. Weeber, C. Chicane, T. David, A. Dereux, and D. Peyrade, Phys. Rev. Lett. **86**, 4950

(2001).

[11] A. Dereux, J. P. Vigneron, P. Lambin, and A. A. Lucas, Phys. Rev. B **38**, 5438 (1988).

[12] O. J. F. Martin, C. Girard, D. R. Smith, and S. Schultz, Phys. Rev. Lett. **82**, 315 (1999).

[13] P. Morse and H. Feshbach, *Methods of Theoretical Physics* (McGraw Hill, New York, 1953).

[14] A. Dereux, Ph.D. thesis, Facultes Universitaires Notre Dame de la Paix, Namur, 1991.

[15] A slightly different definition is also possible. Writing $\delta(k_y'^2 - k_y^2) = 1/2|k_y|[\delta(k_y' - k_y) + \delta(k_y' + k_y)]$, we obtain $\rho(k_y^2) = 1/2k_y[\rho(k_y) + \rho(-k_y)]$ $(k_y > 0)$. Moreover, $\rho(-k_y) = \rho(k_y)$ since $\pm k_y$ simply defines forward and backward propagations. This lead to $\Delta\rho(k_y;\omega) = g/2\pi\Delta k_y/2/(k_y - k_{y0})^2 + (\Delta k_y/2)^2$ instead of Eq. (8) and a degeneracy $g/2$, excluding forward/backward propagation degeneracy.

[16] DOS can also be expressed in the frequency space for fixed momentum k_y. Noticing that θ is a function of both ω and $v = k_y^2$, we use the identity $\frac{\partial\theta}{\partial\omega}|_v \frac{\partial\omega}{\partial v}|_\theta \frac{\partial v}{\partial\theta}|_\omega = -1$ that leads to $\frac{\partial\theta}{\partial\omega}|_{k_y} = -\frac{\partial v}{\partial\omega}|_v \frac{\partial\theta}{\partial v}|_\omega = -2k_y/v_g\pi\Delta\tilde{\rho}(k_y^2;\omega) = -\pi/v_g\Delta\rho(k_y;\omega)$. A Taylor expansion near the resonance frequency ω_0 gives then $\Delta\rho(k_y;\omega) \approx gv_g/\pi\Delta\omega/2/(\omega - \omega_0)^2 + (\Delta\omega/2)^2$, with $\Delta\omega = -2\,\mathrm{Im}\,D(\omega_0;k_y)/[\partial\,\mathrm{Re}\,D(\omega;k_y)/\partial\omega]|_{(\omega=\omega_0)} = 1/\tau = v_g/L_{\mathrm{SPP}}$, and τ is the mode lifetime. See also M. Kretschmann and A. A. Maradudin, Phys. Rev. B **66**, 245408 (2002).

[17] C. Bohren and D. Huffman, *Absorption and Scattering of Light by Small Particles* (John Wiley & Sons, New York, 1983).

[18] G. Colas des Francs, C. Girard, and A. Dereux, J. Chem. Phys. **117**, 4659 (2002).

[19] G. Lévêque, G. Colas des Francs, C. Girard, J.-C. Weeber, C. Meier, C. Robilliard, R. Mathevet, and J. Weiner, Phys. Rev. E **65**, 036701 (2002).

[20] M. Paulus and O. J. F. Martin, Phys. Rev. E **63**, 066615 (2001).

[21] A. V. Krasavin and A. V. Zayats, Appl. Phys. Lett. **90**, 211101 (2007).

[22] T. Holmgaard, S. Bozhevolnyi, L. Markey, and A. Dereux, Appl. Phys. Lett. **92**, 011124 (2008).

[23] J. Grandidier, S. Massenot, G. Colas des Francs, A. Bouhelier, J.-C. Weeber, L. Markey, A. Dereux, J. Renger, M. U. González, and R. Quidant, Phys. Rev. B **78**, 245419 (2008).

[24] E. D. Palik, *Handbook of Optical Constants of Solids* (Academic Press, New York, 1998).

[25] A. Drezet, A. Hohenau, D. Koller, A. Stepanov, H. Ditlbacher, B. Steinberger, F. Aussenegg, A. Leitner, and J. Krenn, Mater. Sci. Eng., B **149**, 220 (2008).

[26] G. Boudebs, S. Cherukulappurath, M. Guignard, J. Troles, F. Smektala, and F. Sanchez, Opt. Commun. **230**, 331 (2004).

[27] R. Quidant, J.-C. Weeber, A. Dereux, D. Peyrade, G. Colas des Francs, C. Girard, and Y. Chen, Phys. Rev. E **64**, 066607 (2001).